Central Washington University
ScholarWorks@CWU

Faculty Scholarship for the Cascadia Hazards Institute

Cascadia Hazards Institute

4-2010

Intensity, Magnitude, Location, and Attenuation in India for Felt Earthquakes since 1762

Walter Szeliga
Central Washington University, walter@geology.cwu.edu

Susan Hough

Stacey Martin

Roger Bilham

Follow this and additional works at: http://digitalcommons.cwu.edu/chifac

Part of the Geology Commons

Bulletin of the Seismological Society of America

Ⓔ

Intensity, Magnitude, Location, and Attenuation in India for Felt Earthquakes since 1762

by Walter Szeliga, Susan Hough, Stacey Martin, and Roger Bilham

Abstract A comprehensive, consistently interpreted new catalog of felt intensities for India (Martin and Szeliga, 2010, this issue) includes intensities for 570 earthquakes; instrumental magnitudes and locations are available for 100 of these events. We use the intensity values for 29 of the instrumentally recorded events to develop new intensity versus attenuation relations for the Indian subcontinent and the Himalayan region. We then use these relations to determine the locations and magnitudes of 234 historical events, using the method of Bakun and Wentworth (1997). For the remaining 336 events, intensity distributions are too sparse to determine magnitude or location. We evaluate magnitude and location accuracy of newly located events by comparing the instrumental- with the intensity-derived location for 29 calibration events, for which more than 15 intensity observations are available. With few exceptions, most intensity-derived locations lie within a fault length of the instrumentally determined location. For events in which the azimuthal distribution of intensities is limited, we conclude that the formal error bounds from the regression of Bakun and Wentworth (1997) do not reflect the true uncertainties. We also find that the regression underestimates the uncertainties of the location and magnitude of the 1819 Allah Bund earthquake, for which a location has been inferred from mapped surface deformation. Comparing our inferred attenuation relations to those developed for other regions, we find that attenuation for Himalayan events is comparable to intensity attenuation in California (Bakun and Wentworth, 1997), while intensity attenuation for cratonic events is higher than intensity attenuation reported for central/eastern North America (Bakun *et al.*, 2003). Further, we present evidence that intensities of intraplate earthquakes have a nonlinear dependence on magnitude such that attenuation relations based largely on small-to-moderate earthquakes may significantly overestimate the magnitudes of historical earthquakes.

Online Material: Table and figures depicting hypocenter locations with supporting parameters and uncertainty.

Introduction

Despite a written history extending more than three millenia, the location and magnitude of earthquakes in the Indian subcontinent and its surroundings prior to 1900 remain largely unquantified. The Martin and Szeliga (2010) catalog of 8339 felt reports of 570 earthquakes since 1636 permits this shortcoming to be addressed. More than 98% of the earthquakes in the Martin and Szeliga (2010) catalog occurred after 1800 and more than 50% since 1900. In this article, we quantify attenuation versus distance relationships for India, and from these we determine the probable magnitudes and locations of earthquakes that occurred before the instrumental catalog.

Previous studies have undertaken similar investigations using less complete data with variable and uncertain quality.

In 1996, Johnston (1996) used published intensity values to derive attenuation parameters for the Indian subcontinent. However, these intensity values were not consistently determined and were biased by the inclusion of observations influenced by liquefaction and by inattention to the effects of building fragility, as was common to early reports. From these data, Johnston (1996) derived relations between isoseismal area and earthquake magnitude.

More recently, a number of studies have carefully and systematically reinterpreted available macroseismic data for a number of important historical earthquakes. Ambraseys and Jackson (2003) present intensity evaluations and approximate magnitudes for several early events in the Himalaya

and southern Tibet (from the years 1411, 1505, 1555, 1713, 1751, 1803 and 1806). Ambraseys (2004) assigns intensity values for a Bangladesh earthquake in 1664 and discusses the location of an earthquake in Sindh in 1668. Ambraseys and Douglas (2004) present reevaluated intensities from 43 earthquakes in northern India and use inferred felt areas to estimate attenuation.

Recent events, such as the 2001 Bhuj earthquake, have been the subject of extensive, traditional, ground-based intensity surveying of damage and other effects (Pande and Kayal, 2003). Additionally, Internet-based methods (Wald et al., 1999a; Amateur Seismic Centre [see Data and Resources section]) have now begun to yield objectively determined intensity distributions for moderate and large earthquakes through the use of standardized questionnaires.

Recent efforts notwithstanding, systematically and carefully determined intensities have remained lacking for both moderate historical earthquakes and for most moderate and large instrumentally recorded earthquakes in India. The new Martin and Szeliga (2010) catalog of felt earthquakes and intensities, compiled from extant records in colonial libraries and newspaper accounts, provides a new, rich source of information for the past two centuries. Intensity values in this catalog were assessed from the original sources using the European Macroseismic Scale 1998 (EMS-98; Grünthal and Levret, 2001). This new catalog includes 234 historical earthquakes, ranging in magnitude from 4 to 8.6, that we judge to have a sufficient number of intensity observations to permit the evaluation of their epicentral parameters. in the electronic supplement The results of these evaluations are shown Ⓔ in the electronic edition of *BSSA*.

This important new catalog provides the basis for determining intensity attenuation relations for India and for determining locations and magnitudes for historical events for which sufficient macroseismic information exists. We conclude our study by discussing examples of four earthquakes from the nineteenth century.

Data and Methods

The intensity values from the Martin and Szeliga (2010) catalog used to derive the attenuation relationships for this study reveal significant scatter at all distances. Although some of this scatter is expected to result from imprecision in intensity assignments (e.g., where structural fragility cannot be adequately assessed), rich, objectively determined intensity distributions (e.g., Wald et al., 1999b; Atkinson and Wald, 2007) reveal that intensities do vary substantially as a consequence of local site geology and other factors. Because there are unknown variations in the precise location of repeated observations, the calculation of meaningful site corrections is not possible. We thus do not consider site corrections in our analysis.

Previous studies of intensity attenuation in the Indian subcontinent have used methods based on the area contained within a contour of specific intensity (e.g., Johnston, 1996;

Ambraseys and Douglas, 2004). These methods assign epicentral locations and magnitudes based on the location of maximum shaking and the areal extent of isoseismal contours. In this study, we use the method of Joyner and Boore (1993) to empirically derive intensity attenuation relationships for the Indian subcontinent. The functional form of the intensity attenuation relationship used in this study is as follows:

$$I = a + bM_\text{w} + cR + d\log(R), \qquad (1)$$

where R is the hypocentral distance, M_w is the moment magnitude, and a, b, c, and d are constants to be determined. Equation (1) is derived by assuming that intensity is logarithmically proportional to the energy density of a point source (Howell and Schultz, 1975). The cR and $d\log(R)$ terms are generally taken to reflect intrinsic attenuation and geometrical spreading, respectively, although in practice these two terms are difficult to resolve independently.

A one-stage maximum-likelihood methodology is used to derive the intensity attenuation relationship using 29 calibration events (Joyner and Boore, 1993). Our calibration events consist of earthquakes since 1950 with more than 15 felt-intensity reports (Fig. 1). Although we give preference to earthquakes with hypocenters in the Centennial Catalog (Engdahl and Villasenor, 2002), we utilize other hypocentral catalogs for more recent earthquakes. If an event is not listed in the Centennial Catalog, we use hypocentral estimates from the *Bulletin of the International Seismological Centre* (ISC) and thereafter, the USGS National Earthquake Information Center Monthly Hypocenter Data File (MHDF). Preferred moment magnitude estimates are from the Global Centroid Moment Tensor Project (CMT). If an event is not listed in the
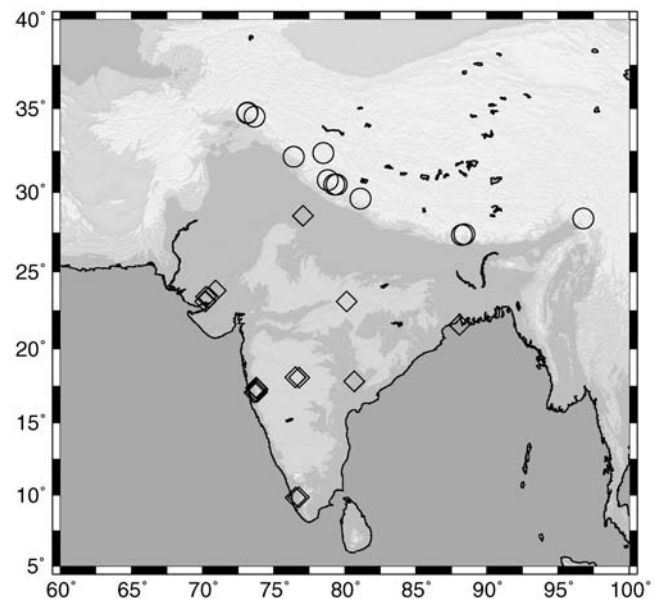
Figure 1. Epicentral locations of 29 calibration events. We have excluded earthquakes with depths in excess of 40 km. Diamonds, events used to determine cratonic attenuation; circles, events used to determine Himalayan attenuation.

Global CMT, we use moment magnitude estimates from the Centennial Catalog, ISC, or the MHDF, in decreasing order of preference (see Data and Resources section). For five calibration events $(4.1 < M < 5.3)$, only body-wave magnitude (m_b) estimates were available. Converting these body-wave magnitudes to moment magnitudes using a published linear relationship resulted in attenuation relationship coefficients that were statistically indistinguishable from the uncorrected magnitudes. We therefore have chosen to retain the original body-wave magnitudes during inversion. For the largest event in the catalog, the 1950 Chayu earthquake in eastern Assam, we use the hypocentral location and magnitude listed in Chen and Molnar (1977).

We first use a least squares approach to estimate parameters $a - d$ in equation (1), using the magnitude of all calibration earthquakes as well as the hypocentral distance to each observation. The least squares inversion is weighted by a covariance matrix that includes off-diagonal terms that account for intraearthquake observational variance. The inversion is performed by inverting the normal equations with the off-diagonal terms in the covariance matrix being determined using a maximum-likelihood methodology.

Utilizing the attenuation relation derived from the methods outlined previously, we then use the method outlined in Bakun and Wentworth (1997) to determine epicenters and magnitudes. For each earthquake we create a $5° × 5°$ grid of trial hypocenters centered on the instrumentally determined hypocenter with a grid spacing of 5 arc-minutes. If no instrumental hypocenter is available, we use the geometrical centroid of all of the intensity observations weighted by their EMS-98 value and a depth of 15 km. For each trial hypocenter, we calculate the slant distance to each intensity observation and solve equation (1) for M_w. A weighted measure of the dispersion of the magnitude estimates is then calculated at each grid point using the following equation:

$$\sigma = \left(\frac{\sum_i (W_i (M_i - \bar{M}))^2}{\sum_i W_i^2} \right)^{\frac{1}{2}} \quad (2)$$

with

$$W_i = \begin{cases} 0.1 + \cos\left(\frac{\Delta_i \pi}{(2)(150)}\right) & \Delta_i < 150 \text{ km} \\ 0.1 & \Delta_i > 150 \text{ km} \end{cases},$$

where Δ_i is the distance from the trial hypocenter to each intensity observation i, M_i is the magnitude estimated from equation (1) for observation i, and $\bar{M}$ is the mean magnitude

at the trial epicenter. We then choose the trial epicenter that minimizes equation (2) as the preferred epicentral estimate and its associated $\bar{M}$ as the preferred magnitude estimate. In a scenario where all intensity observations are given equal weight, (i.e., choosing $W_i = 1.0$ for all Δ_i), equation (2) becomes the sample standard deviation. Thus, the trial epicenter that minimizes equation (2) will be referred to as the minimum deviation epicenter.

In general, intensity observations show a rapid decay close to the epicenter; this behavior indicates that intensity observations near the epicenter are more sensitive to the epicentral location and magnitude than are observations farther away. Thus, we choose a function, W_i, that gives greater weight to observations that are closer to the trial epicenter. While Bakun and Wentworth (1997) note that the 150 km cutoff distance chosen for the weighting function is arbitrary, we retain this value to facilitate direct comparison of our results with those of Bakun and Wentworth (1997). A possible benefit of retaining a cutoff distance of 150 km is that it down-weights potentially magnified observations that may result from critically reflected seismic phases, such as SmS. In India, Moho depths vary from greater than 50 km on the craton (Gupta et al., 2003) to 40 km beneath the Himalaya (Monsalve et al., 2008). Given a hypocentral depth of 15 km, one could reasonably expect SmS to first appear between 120 and 150 km from an epicenter.

Results

We calculate separate attenuation parameters for earthquakes in the subcontinent (craton) and the Himalaya, in addition to evaluating the parameters for the entire data set (Table 1). Additionally, Figure 2 shows the distribution of intensity data used to calculate the attenuation parameters as a function of moment magnitude.

To investigate the self-consistency of our results, we utilize a cross-validation scheme (Efron and Tibshirani, 1993) to characterize the predictive ability of our data set. We determine attenuation relationships using subsets of 21 instrumentally recorded calibration events randomly chosen without replacement from our original list of 29 calibration events. We then use the resulting attenuation relationship to determine the locations and magnitudes of the remaining eight calibration events. This procedure is repeated to create 100 cross-validation samples. The resulting statistics show a median epicentral misfit of 53 km and a magnitude misfit of 0.38 M_w.

Table 1

Intensity Attenuation Relationship Parameters for India, the Indian Craton, and the Himalaya

Province	Number of Events	a^*	b^*	c^*	d^*
India	29	5.57 ± 0.58	1.06 ± 0.07	-0.0010 ± 0.0004	-3.37 ± 0.25
Craton	17	3.67 ± 0.79	1.28 ± 0.10	-0.0017 ± 0.0006	-2.83 ± 0.30
Himalaya	12	6.05 ± 0.94	1.11 ± 0.10	-0.0006 ± 0.0006	-3.91 ± 0.38

*Columns a, b, c, and d refer to the variables in equation (1).
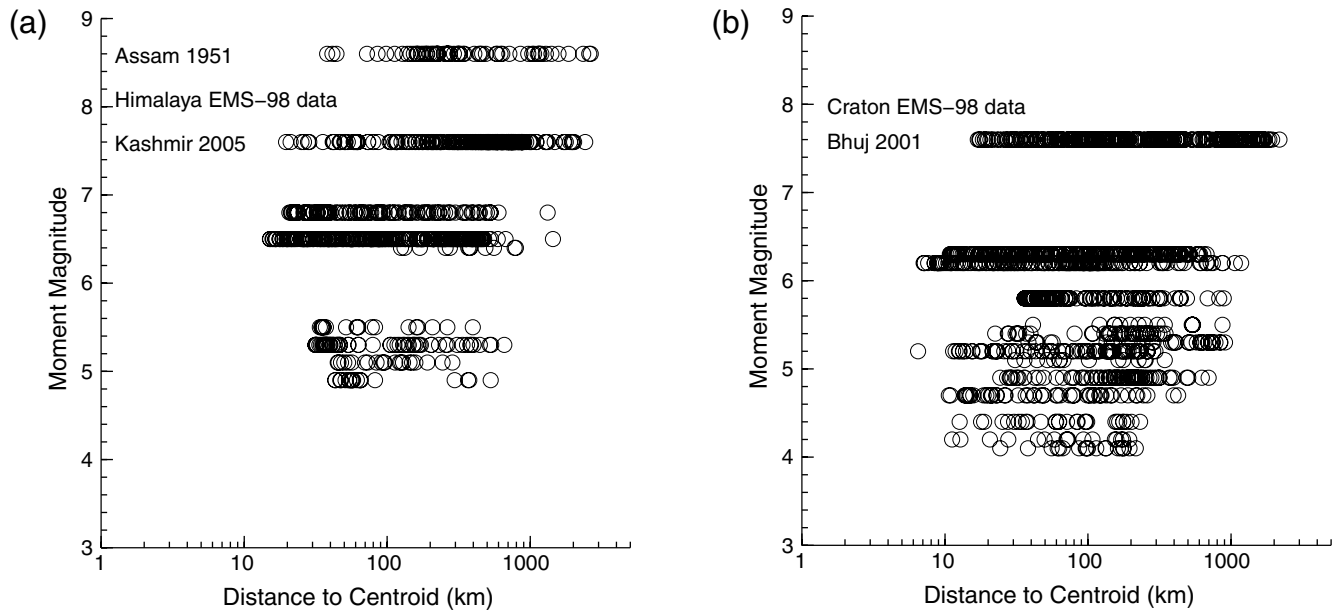
Figure 2. Intensity distributions for the data used to calculate the attenuation parameters in Table (1). (a) Distance to earthquake centroid versus moment magnitude for events in the Himalaya. (b) Distance to earthquake centroid versus moment magnitude for events on the craton.

Comparisons with Previous Attenuation Studies

As noted, previous macroseismic studies in the Himalaya have used the areal extent of isoseismal radii to develop attenuation relationships (Ambraseys and Douglas, 2004). Figure 3 shows a comparison of these results with the attenuation relationship developed here for the Himalaya.

While the attenuation relationship developed in this study disagrees with that derived by Ambraseys and Douglas (2004) at the $2 - \sigma$ level (Table 2), the two attenuation relationships are not grossly inconsistent for intensities greater than IV. Both relationships appear to parallel each other before diverging below intensity III. We consider the sharp divergence between these relationships below intensity III to be caused by differences in the definition of the radius of perceptibility between the EMS-98 scale and the Medvedev–Sponheuer–Karnik (MSK) scale. In fact, the two attenuation relationships can be brought into excellent agreement by either decrementing the value of a in our study by 0.5 intensity units or decreasing the epicentral distance by 25 km. Reasons for this shift between the relationships could include the use of half-unit intensities in Ambraseys and Douglas (2004), a slight bias in assessed intensities between the two studies, variations in the precision of the epicentral locations of the calibration events between the studies, and differences in the methodology used to calculate the calibration curves.

Of these possibilities, we can only test for the presence of a bias between the two data sets. We have compiled a direct comparison of 95 intensities from three earthquakes with common locations in both the Martin and Szeliga (2010) catalog and Ambraseys and Douglas (2004) (Fig. 4). This comparison indicates that the two studies are in good statistical agreement, with more than 88% of the assessed

intensities differing by no more than one intensity unit. Although none of these earthquakes are used in the generation of the calibration curves in Martin and Szeliga (2010) and most assessed intensities are identical between studies (ΔIntensity $= 0$), this comparison shows that there appears to be a slight bias toward lower values in the Martin and Szeliga (2010) catalog by no more than one intensity unit. Because a bias toward lower values in intensities in the Martin and Szeliga (2010) catalog would require incrementing the value of a, we may rule out the possibility that a systematic bias is responsible for the discrepancy between the two attenuation relationships.
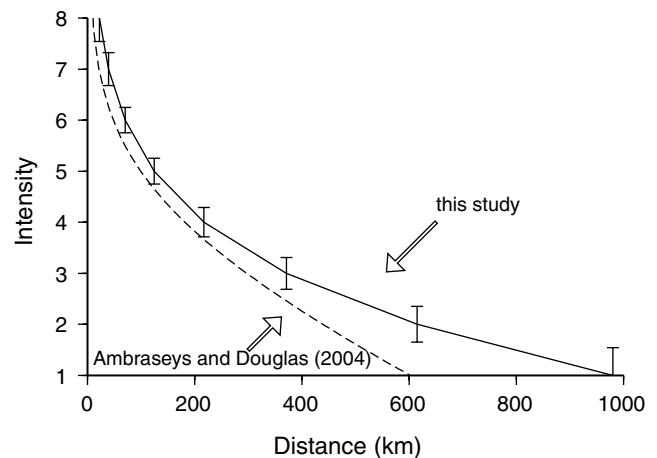

Figure 3. Intensity attenuation with distance for a hypothetical M 6.5 Himalayan earthquake from this study (solid line) and from Ambraseys and Douglas (2004) (dashed line). Intensity data from this study are in EMS-98, and data from Ambraseys and Douglas (2004) are in MSK. Error bars are $2 - \sigma$. (See Table 2.)
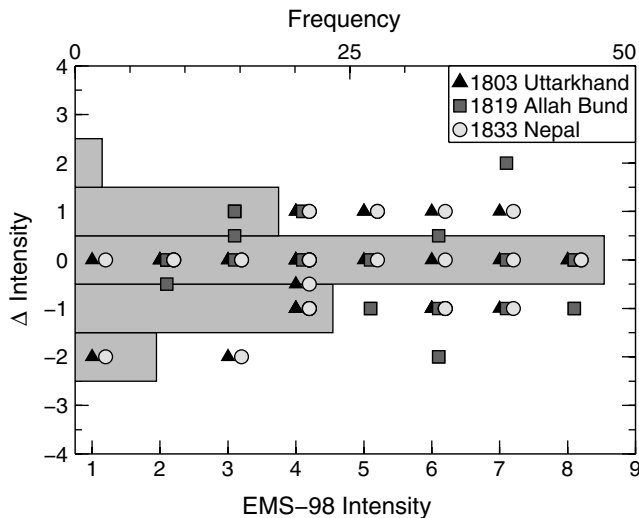
Figure 4.   Comparison of assessed intensities at 95 common locations from Martin and Szeliga (2010) and Ambraseys and Douglas (2004) for three earthquakes. The *x*-axis (top) corresponds to the normalized frequency of the combined intensity differences. For individual earthquakes, the *x*-axis (bottom) corresponds to the assessed intensity value from the Martin and Szeliga (2010) catalog. The *y*-axis corresponds to the difference between the assessed intensities from Martin and Szeliga (2010) and those from Ambraseys and Douglas (2004), with negative values indicating that the intensity from Martin and Szeliga (2010) is lower than that listed in Ambraseys and Douglas (2004). For clarity, intensities for the 1819 Allah Bund and 1833 Nepal earthquakes have been artificially offset to the right by 0.1 and 0.2 intensity units respectively.

It has generally been assumed, based on overall similarities between the crustal structure and age of eastern North America and India, that the regions are characterized by similar attenuation of seismic waves and intensities (Johnston, 1996; Talwani and Gangopadhyay, 2000; Ellis *et al.*, 2001). However, previous authors have inferred systematic differences in both peak ground motion attenuation and weak-motion attenuation between eastern North America and other stable continental regions worldwide (Bakun and McGarr, 2002; Miao and Langston, 2008). Both Bakun *et al.* (2003) and Atkinson and Wald (2007) have developed relationships between intensity and epicentral distance for eastern North America (Table 2). Figure 5 compares intensity attenuation relationships in India with those from eastern North America for a hypothetical M_w 6.5 earthquake. For all epicentral distances, the attenuation relationship of Bakun *et al.* (2003) predicts higher intensity observations in eastern North American compared to cratonic India. In contrast, the relationship developed by Atkinson and Wald (2007) agrees with that for cratonic India above intensity V but below intensity V, and these two relationships diverge sharply, with larger intensity values being predicted to greater distances in eastern North America. This could be due to differences in gross crustal properties between eastern North American and cratonic India such that higher-mode surface waves (*Lg*) travel more efficiently in eastern North America. However,
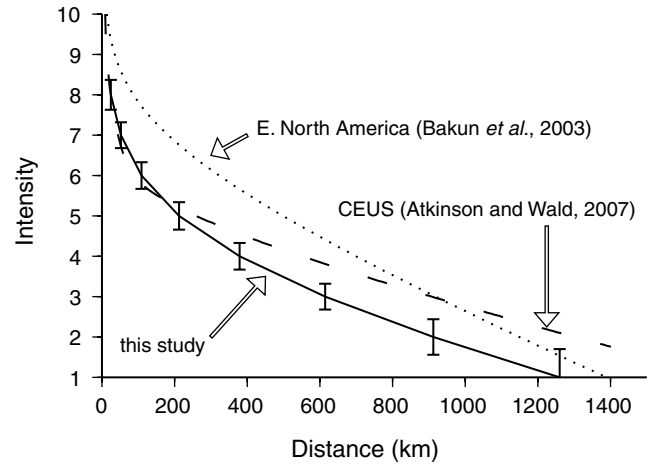

Figure 5.   Comparison of the intensity attenuation relationships from this study for India, from Bakun *et al.* (2003) for eastern North America, and from Atkinson and Wald (2007) for the central eastern United States (CEUS) for a hypothetical *M* 6.5 earthquake. Indian intensity data are in EMS-98, while data from eastern North America are in Modified Mercalli Intensity (MMI). Error bars are $2 - \sigma$. (See Table 2.)

we note that Atkinson and Wald (2007) assume a different functional form for intensity attenuation, one that includes nonlinear magnitude terms.

A comparison of our results with the results of Bakun *et al.* (2003) could be complicated by uncertainties associated with their results. In particular, the intensity values for calibration events used by Bakun *et al.* (2003) have not been systematically reinterpreted and may suffer from the same problems that formerly plagued available intensity values for India. To further investigate the difference revealed in Figure 5, we directly compare attenuation from earthquakes of similar magnitude in eastern North America and cratonic India. For low magnitude earthquakes ($M \sim 4.5$), the median distance at which shaking of intensity III and IV is felt is twice as far in eastern North America as compared with cratonic India (Fig. 6). These direct comparisons corroborate the result that attenuation is at least a factor of 2 lower in eastern North America compared to cratonic India.

While both the Himalaya and California are active plate boundary zones, there is no reason to expect good agreement in intensity attenuation between the two regions. Nonetheless it is interesting to compare the results for these two regions. Our results suggest that intrinsic attenuation is small ($c = -0.0006$ in equation 1) in the Himalayan region, which is in agreement with the results of Atkinson and Wald (2007) (their equivalent of *c* has a value of -0.0007), while Bakun and Wentworth (1997) developed the California relationship using 22 calibration events under the assumption that intrinsic attenuation was negligible ($c = 0$ in equation 1) (Table 2). This low intrinsic attenuation is indicative of a highly absorptive crust (high attenuation, low *Q*) which is expected in a tectonically active region. Allowing for a vertical shift of up to 0.5 intensity units due to differences in the intensity
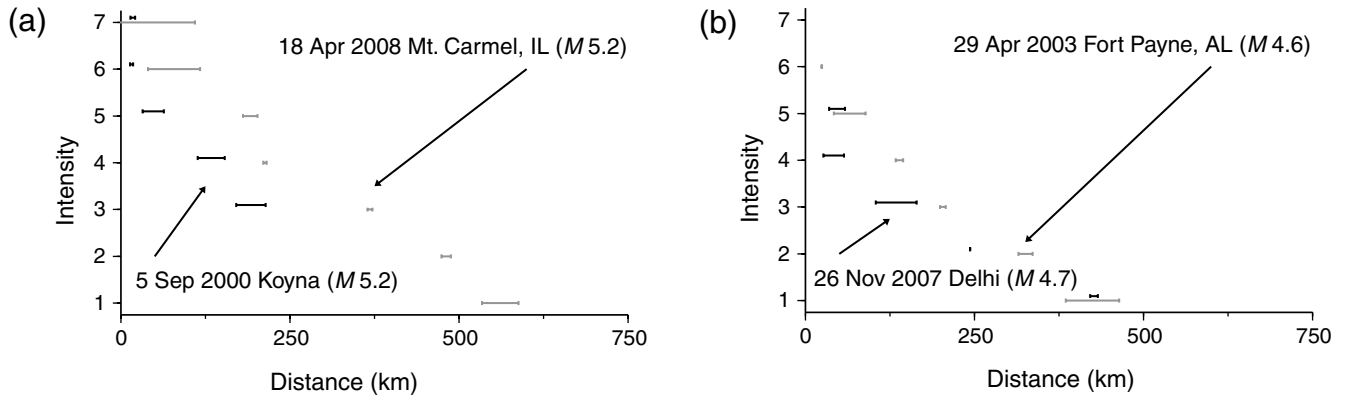
Figure 6. A direct comparison of intensity observations between eastern North America and cratonic India. Eastern North American intensity data are from the USGS Community Internet Intensity Map Project; error bars represent standard error estimates of the sample median. (a) Direct comparison of the median distance to which each intensity was observed for the 18 April 2008 M_w 5.2 Mt. Carmel, Illinois, earthquake and the 5 September 2000 M_w 5.2 Koyna earthquake. For intensities III–VI, the median distance is statistically larger for the Mt. Carmel, Illinois, earthquake. (b) Direct comparison of the median distance to which each intensity was observed for the 29 April 2003 M_w 4.6 Fort Payne, Alabama, and the 26 November 2007 M_w 4.7 Delhi earthquake. Although the Delhi earthquake is larger than the Fort Payne earthquake, the median distance to which intensities II–V are felt is smaller in India. This suggest that the attenuation difference between eastern North American and India is equivalent to a magnitude increase of at least 0.2 M_w.

scales utilized, Figure 7 illustrates remarkably good agreement between both the Californian and the Himalayan intensity attenuation relationships.

### Estimation of Historical Epicenters and Magnitudes

The precise locations of historical earthquakes in India and the Himalaya have important consequences for recurrence interval studies as well as seismic hazard assessment. Using the intensity attenuation relationships derived in the preceding section, we determine the locations and magnitudes of historical events, examine the uncertainties of epi-

Figure 7. Intensity attenuation relationships for the Himalaya from this study, the results of Bakun and Wentworth (1997) for California, and the results from Atkinson and Wald (2007) for California for a hypothetical M 6.5 earthquake. Indian intensity data are in EMS-98 while data from California are in MMI. (See Table 2.)

central locations and magnitudes, assess the completeness of our catalog, and take a closer look at four historical earthquakes that have previously been interpreted as great earthquakes. Maps showing the location and magnitude of historical earthquakes calculated using data from the Martin and Szeliga (2010) catalog are shown Ⓔ in the electronic edition of *BSSA*. Finally, we use the intensity distribution for the 2001 Bhuj earthquake to investigate what one would infer for this event had it been known only from historical sources.

Epicentral Locations and Magnitudes of Historical Events

For earthquakes prior to 1890, the only information available to us for assessing the location and magnitude of most historical earthquakes in India comes from felt-intensity data. The exceptions are for those earthquakes whose location can be constrained from independent observations such as tide gauge data (e.g., the 1881 Car Nicobar earthquake; Ortiz and Bilham, 2003), documented surface rupture (e.g., the June 1505 central Himalayan earthquake for which surface slip has been measured; Yule, personal commun, 2007), and obvious surface deformation (e.g., the 1819 Allah Bund earthquake; Oldham, 1926), which caused local uplift and a large region of subsidence).

The Martin and Szeliga (2010) catalog affords us the possibility of refining both the location and magnitude of many earthquakes in the historical record. Although the approach outlined in Data and Methods offers a sophisticated method to quantitatively evaluate a probable epicentral location and, with it, a probable magnitude, we have found that the Bakun and Wentworth (1997) algorithm frequently chooses erroneous values where the results can be compared with instrumental values. For 100 test earthquakes for which we have
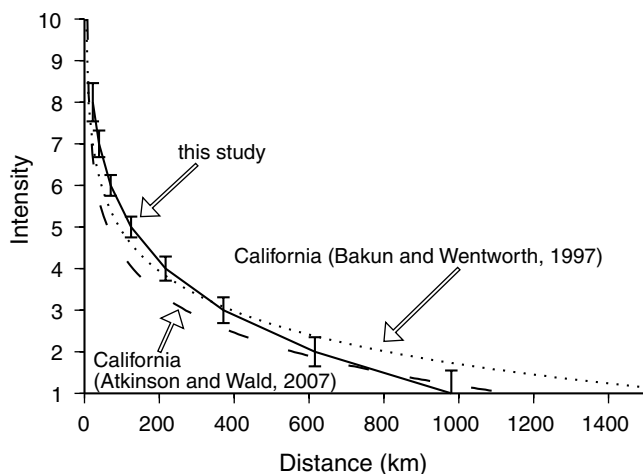
both intensity data and an instrumental location and magnitude, the median location error is 120 km with a median magnitude overprediction error of M_w 0.4.

The reason for the errors in location follows partly from a paucity of observations and their spatial coverage, partly from the absence of a large range of intensity values in a given earthquake, and partly from the measure of dispersion chosen as our metric in equation (2). Even for some very well-recorded earthquakes that do not have these shortcomings, the estimated epicentral location is often counterintuitive and, where we can test its true location, demonstratively incorrect. Examples are discussed subsequently. It may be possible to decrease the discrepancies in epicentral location and magnitude by choosing a measure of dispersion that is more robust than equation (2) in the presence of outliers.

Where azimuthal felt-intensity coverage is limited to one quadrant or to two contiguous quadrants from the epicenter, as, for example, in earthquakes near the coast or on the southern edge of the Tibetan plateau (where reporting is inevitably one sided), there is often a trade-off between magnitude and location. We found that location accuracy in such cases can be improved by selecting the preferred hypocentral location to coincide with the location of the minimum magnitude, $\bar{M}$, from equation (2). This minimum magnitude location rarely corresponds to the minimum deviation location determined using equation (2). Lest too much credibility be attached to the coordinates derived from the minimum deviation solution, we also list coordinates for the minimum magnitude in Ⓔ Table S1 of the electronic edition of *BSSA*. The mean location error using the minimum magnitude location as a conservative constraint more than halves the misfit for the

100 test earthquakes to 44 km in position; however, this method also systematically underpredicts earthquake magnitudes by M_w 0.6.

As an example, we show the location errors from the minimum deviation method for aftershocks following the 10 December 1967 Koyna earthquake and nearby earthquakes (Fig. 8a). Some earthquakes were misplaced out to sea, or far inland, with a median mislocation error of 120 km. For some aftershocks, magnitudes are estimated to be larger than the mainshock. In contrast, the location of the minimum magnitude yields a median mislocation error of 26 km (Fig. 8b), with magnitudes that were within 0.35 M_w of their instrumental values. For earthquakes with more than 100 felt observations, the location error is less than or equal to the grid spacing (~9 km).

While it is clearly to some extent a subjective decision whether to use the minimum magnitude or the minimum deviation solution, we note that choosing the minimum magnitude is consistent with the probability that, had the magnitude been larger, in many cases it would have been felt by people in other quadrants.

In a search for a simple discriminant to reject aberrant solutions, we found that the most accurate locations (within 30 km of the epicenter) are those for which the locations chosen by equation (2) and the minimum magnitude location differ by less than 30 km. However, if one were to apply this criterion strictly, one would reject the locations of more than two-thirds of the earthquakes. We prefer to include solutions for a larger set of events, but it is important to note the uncertainties discussed previously when utilizing our solutions.
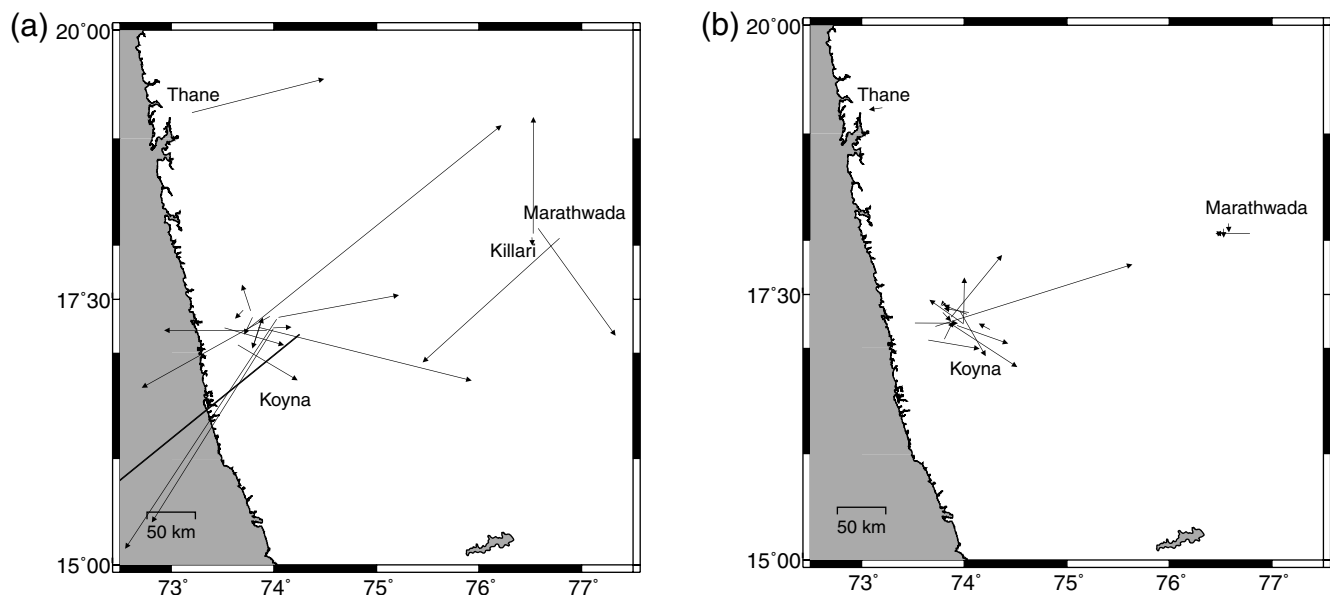
Figure 8. Comparison of the epicentral misfit for instrumentally recorded earthquakes in the Koyna region of India. On both figures, the arrow points from the instrumental epicenter toward the intensity-derived epicenter. (a) Epicentral misfit in the Koyna region using the location of the minimum of equation (2) as the epicentral estimate. (b) Epicentral misfit in the Koyna region using the location of the minimum $\bar{M}$ from equation (2).

Catalog Completeness

Using the magnitudes we have calculated for 234 events in the Martin and Szeliga (2010) catalog, we compare their magnitude distribution to the magnitude distribution from the ISC catalog covering the same geographic region during the period 1980–2000 (Fig. 9, see Data and Resources section). Two first-order observations are apparent: (1) the earthquake listing in the Martin and Szeliga (2010) catalog appears to be significantly incomplete even for M_w 7.5, and (2) there appear to be too many earthquakes with $M_w > 8$.

To investigate the extent to which missing aftershocks from large earthquakes might be responsible for the incompleteness of the catalog below M_w 7.5, we remove known aftershocks from the catalog. Then for each earthquake, we add aftershocks according to a Gutenberg–Richter distribution (Gutenberg and Richter, 1954), with the largest aftershock in each sequence being 1.2 units smaller than its mainshock (Båth, 1965). The resulting distribution is significantly closer to the distribution inferred from the ISC catalog, although the distribution of events still appears to be incomplete by a factor of 3 for M_w 7, and a factor of 5 for M_w 5.

The overabundance of earthquakes with $M_w > 8$ is likely due to tendency of the minimum deviation method to overpredict magnitude by nearly M_w 0.4. Although some of the catalog incompleteness above M_w 7 could be remedied by adjusting higher magnitudes downward, it is impossible to determine precisely which historical earthquakes have inflated magnitudes. As a result, it is not possible to correct for this bias. However, this bias cannot account for missing earthquakes with $M_w < 6$; we therefore conclude that a substantial number of earthquakes are missing from the historical record. This result is not surprising, given the especially
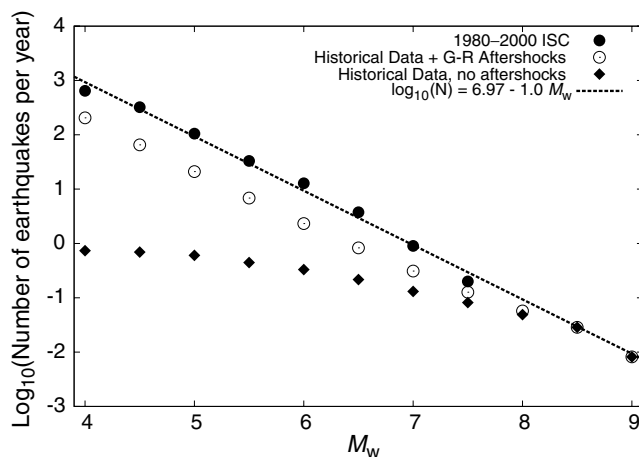
Figure 9. Frequency–magnitude plot of earthquakes occurring on the Indian subcontinent. Filled circles, events from the ISC catalog during 1980–2000; diamonds, events from the Martin and Szeliga (2010) catalog; open circles, with synthetic aftershock sequences from a Gutenberg–Richter distribution added as described in section "Catalog Completeness"; dashed line represents a frequency–magnitude relationship with a b value of 1.0.

scanty early historical record that is available for some of the remote parts of our study area. Nonetheless, assuming it is reasonable to include missing aftershocks, the distribution of magnitudes provides a basis for quantification of overall earthquake rates for seismic hazard assessment.

Recent studies have identified surface scarps that appear to have been generated by extremely large megathrust earthquakes (e.g., Lavé *et al.*, 2005; Kumar *et al.*, 2006). One can use the inferred magnitude-frequency distribution to explore the expected rate of events that are larger than those in the historical record. Using a maximum-likelihood method (Bender, 1983) to fit the ISC results for $M_w \leq 7.5$ and our results for larger events, we infer $\log_{10}(N) = 7.17 - 1.034M$. Although at some point one expects a simple linear extrapolation to not be valid, this equation predicts one M_w 9.5 event in the region on the order of once every 450 years.

Case Studies

The 1803 Uttarakhand Himalaya Earthquake

On 1 September 1803, a large earthquake shook much of the central Himalaya and nearby Ganges plains, causing severe damage to the town of Uttarkashi (Barahat). This earthquake is famous for its alleged damage to the Qutab Minar in Delhi, a structure that had stood, undamaged, since its construction in the thirteenth century. This earthquake is described briefly by Mallet and Mallet (1858) and Oldham (1883). While Seeber and Armbruster (1981) consider it the first of four great, colonial Himalayan earthquakes, no quantitative evaluation of this earthquakes magnitude was attempted before Ambraseys and Jackson (2003), who compiled intensity reports from over 30 locations and assigned a tentative magnitude of M_S 7.5. Subsequent authors (Ambraseys and Douglas, 2004; Rajendran and Rajendran, 2005) also assigned magnitudes in the mid-7s using both Frankel's method (Frankel, 1994) and an isoseismal area method tailored to India. Ambraseys and Douglas (2004) assign an epicentral location near the Tibetan border (31.5° N, 79.0° E), while Rajendran and Rajendran (2005) assign an epicentral location near Srinagar (Sirmur) based on the region of maximum shaking intensity. Using the methods outlined in Data and Methods, we assign a magnitude of M 7.3 with an intensity center (epicentral location) of 30.656° N, 78.784° E (Fig. 10). Our preferred epicentral location lies 9 km south of the 1991 M 6.8 Uttarkashi earthquake and 65 km west of the 1999 M 6.6 Chamoli earthquake. Our study confirms that this was not a great earthquake, despite it being reported in numerous locations throughout the Ganges Plain. The surprising proximity of the 1803 and 1991 earthquakes is suggestive that one may be a recurrence of the other. In 188 years, the present day convergence rate would result in a slip deficit of greater than 3 m, more than sufficient to drive an M 6.8 earthquake (Jade *et al.*, 2004).

The 1819 Allah Bund Earthquake

The 16 June 1819 Allah Bund earthquake is one of the earliest events with well-documented surface faulting (Oldham, 1926) and was responsible for the formation of Lake Sindri, a 20 km north–south by 30 km east–west basin in the northwestern Rann of Kachchh. Upon formation, the lake flooded the village of Sindri and destroyed a fort of the same name. Simultaneously, a region with 6 km north–south width and with an inferred east–west length of 50–80 km rose and dammed the Puram River for several years before a flood incised the uplifted region and the river reoccupied its old channel. This raised region was named the Allah Bund (literally, dam of God) to distinguish it from the several artificial dams across the Puram River (Oldham, 1926). Although both the amplitude and extent of surface deformation in 1819 has been questioned (Rajendran and Rajendran, 2001), the sense of the observed surface uplift and subsidence provides an approximate constraint on the mechanism and magnitude of the earthquake (7.7 ± 0.2), from which an epicenter several kilometers north of the Allah Bund has been proposed (Bilham, 1998).

Less than 200 years later, the occurrence of a second large earthquake on the Kachchh mainland, the 2001 Bhuj earthquake (M_w 7.6), provided a much denser sampling of over 350 felt reports Martin and Szeliga (2010) and Pande and Kayal, 2003). The similarity of these reports to the felt reports of the 1819 earthquake caused Hough et al. (2002) to conclude that the 1819 and 2001 earthquakes were of similar magnitude. In contrast, Ambraseys and Douglas (2004) list the 1819 earthquake as being much larger (M_w 8.2), although they note that no detailed reevaluation of the earthquake was undertaken.

When applied to the 1819 intensity data, the algorithm outlined in Data and Methods unexpectedly identifies an epicentral location 40 km northeast of the 2001 Bhuj epicenter (Fig. 11). This location is 100 km east of the channel incised through the Allah Bund first described by (Burnes, 1835) and close to the mapped Island Belt fault (Fig. 11). The intensity-based magnitude for the 1819 earthquake is thus larger and the epicenter more to the east than those estimated from geological or geodetic interpretations adopted in previous studies. In contrast to the Koyna aftershocks discussed earlier, the minimum magnitude solution lies south of the Kachchh mainland and is considerably less probable than the epicenter chosen by the method of outlined in Data and Methods, given our current understanding of the regional tectonics.

We find however, that the optimal epicenter is sensitive to the values of intensities assigned to points north of the epicenter. Three of these points are mentioned telegraphically by MacMurdo (1823) and lend themselves to debate. The Martin and Szeliga (2010) catalog conservatively assigns intensity V to the southern two locations based on the statement by MacMurdo that shaking there was less severe
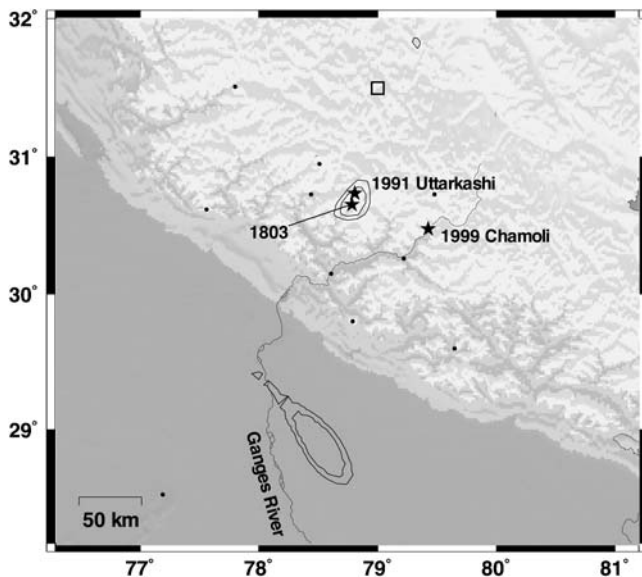
Figure 10. The location of the 1803 Uttarkashi earthquake, as determined by the method outlined in Data and Methods. The contours represent the 50% and 67% confidence contours, as determined by Bakun (1999). The instrumental epicenters of the 1991 Uttarkashi and 1999 Chamoli earthquakes (stars) are shown for reference. The location of the 1803 Uttarkashi earthquake as determined by Ambraseys and Douglas (2004) is illustrated by a square. We reject the alternative epicentral location permitted by the data near the Ganges (indicated by the closed 50% and 67% confidence contours). Filled circles indicate the locations of felt reports for the 1803 earthquake within 250 km of the epicenter.
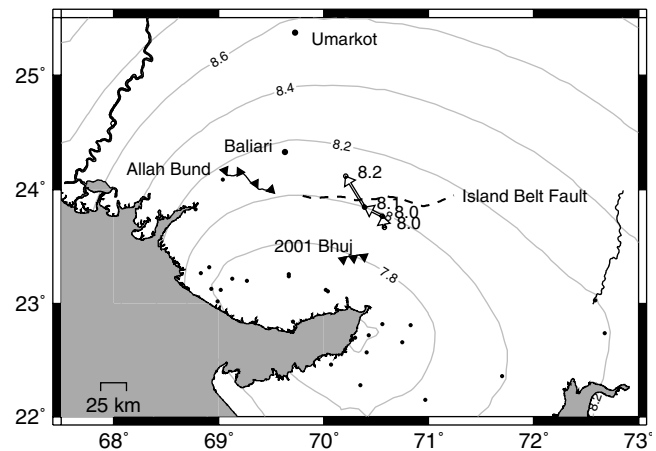
Figure 11. Possible locations for the 1819 Allah Bund earthquake, as determined by the method outlined in Data and Methods (open arrows with calculated M_w). The parameters of these possible locations are listed in Table 3. Black triangles (on the hanging wall), locations of the fault responsible for the 2001 Bhuj M_w 7.6 earthquake (Schmidt and Bürgmann, 2006) and the Allah Bund fault (Malik et al., 2001); dashed line, location of the inferred Island Belt fault (Malik et al., 2001); filled circles, felt-intensity locations within 300 km of the epicenter; arrows, the change in epicentral location due to changes outlined in Table 3. Contours represent magnitudes from the epicentral location algorithm (Data and Methods) using the raw intensity data; they indicate a minimum magnitude location in the Gulf of Kachchh. The locations of Umarkot and Baliari are shown for reference.

Table 2

Intensity Attenuation Relationship Coefficients Obtained by Other Investigations
Used in This Article

Article	Number of Events	a^*	b^*	c^*	d^*
Bakun and Wentworth (1997)	22	3.67	1.17	$0^\dagger$	−3.19
Bakun *et al.* (2003)	28	1.41	1.68	−0.00345	−2.08
Ambraseys and Douglas (2004)	23	0.46	1.54	−0.004	−2.54

*Columns *a*, *b*, *c*, and *d* refer to the variables in equation (1). The form of the attenuation relationship used by Atkinson and Wald (2007) and its associated coefficients are listed in Table (1) and equation (1) in Atkinson and Wald (2007).

†This parameter was defined to be zero.

than on the Kachchh mainland. However, MacMurdo did not personally travel north of the Rann of Kachchh, and damage to masonry forts on the Kachchh mainland near Anjar and Bhuj suggest intensities as high as IX (Bilham, 1998; Ambraseys and Douglas, 2004). Thus, intensities to the north of the epicenter could reasonably be as high as VIII and still remain consistent with MacMurdo's assertion.

Accordingly, we experimentally examined the shift in location caused by increasing the assigned intensities at the two closest locations just north of the Bund (Table 3). The resulting shifts in epicentral location illustrate how sensitive the solution is to the sparse northern data. In each case, the minimum magnitude location lies in the Gulf of Kachchh and yields a magnitude of M_w 7.6. This location can be dismissed as inconsistent both with recent microseismic and tectonic data and with available historical information. As the intensities at Baliari and Umerkot are increased, the preferred epicentral location passes north of the easternmost projection of the Allah Bund, and the magnitude increases, eventually attaining a magnitude of M_w 8.2.

The credibility of these solutions, however, is diminished by the disquieting sensitivity of the solution to intensities north of the Allah Bund and the complete absence of observations to the west. It is doubtful that our knowledge of the shaking intensity at these locations or locations to the west and northwest of the Bund will be significantly improved in the future due to an absence of detailed historical records in the region. Thus, although our analysis using the

Table 3

Epicentral Locations and Intensity Magnitudes (M_I) of the 1819 Allah Bund Earthquake Determined Using the Method Outlined in Data and Methods*

Latitude	Longitude	Depth (km)	M_I	EMS-98	
				Baliari	Umarkot
23.67	70.58	15.00	8.0	5	5
23.77	70.56	15.00	8.0	6	6
23.85	70.39	15.00	8.1	7	6
24.12	70.21	15.00	8.2	8	7

*Uncertainty in descriptions of damage to the towns of Baliari and Umarkot in MacMurdo (1823) permit a range of EMS-98 intensities, with a resulting range in the epicentral location and magnitude for the 1819 earthquake (Fig. 11).

methods outlined in the Data and Methods section favors $8.0 \le M_w \le 8.2$ and a location to the east of the Allah Bund, we are skeptical of the result due to deficiencies in the observations. Of note, however, is the result that the magnitude corresponding to the minimum deviation location appears to overestimate the probable true magnitude.

The 1833 and 1866 Nepal Earthquakes

On 26 August 1833, three earthquakes shook the Kathmandu Valley—the first sufficiently alarming to bring people out of doors, the second (5 hours later) alarming enough to keep them there, and the third (occurring just 15 minutes later) being the most destructive. Bilham (1995) estimated the 1833 mainshock to be 7.7 ± 0.2 using the methods of Johnston (1996), while Ambraseys and Douglas (2004) calculate a magnitude of M_w 7.6 with an epicenter 40 km east of Kathmandu (27.7° N, 85.7° E). We infer a preferred magnitude of M 7.3 ± 0.1 with a location nearly 80 km east–southeast of Kathmandu (27.553° N, 85.112° E) (Fig. 12). Our calculated location roughly corresponds to the location inferred by Bilham (1995); however, our calculated magnitude is smaller than that inferred by both Bilham (1995) and Ambraseys and Douglas (2004). Although epicenters for the two foreshocks are poorly constrained, using the assumption that they occurred within the source region of the main shock yields magnitudes of M 5.1 and M 6.5 respectively.
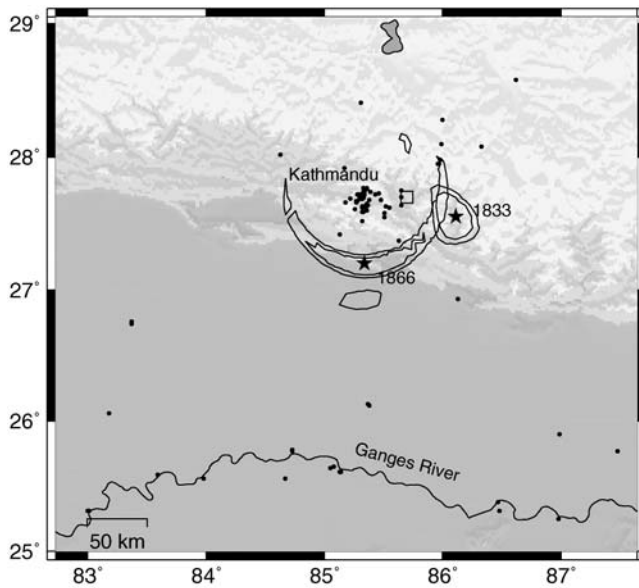
A moderate earthquake occurred on 23 May 1866 near Kathmandu that is mentioned by several authors (Oldham, 1883; Khattri and Tyagi, 1983; Khattri, 1987; Rajendran and Rajendran, 2005). Khattri (1987) assesses the magnitude of the 1866 event as M 7.6, based on rupture length–magnitude scaling relationships (Wyss, 1979). Although our epicentral location is poorly constrained due to a lack of observations north of Kathmandu, our data are consistent with an epicentral location within 80 km of Kathmandu and a magnitude of 7.2 ± 0.2 (Fig. 12). Thus, according to our intensity analysis, the 1833 and 1866 earthquakes both appear to have ruptured similar locations in the Nepal Himalaya with similar magnitudes. In this case, unlike the 1803/1991 earthquake pair, the slip in the second event would not have developed over the course of 33 years with a geodetic convergence rate of 18 mm/yr (Jade *et al.*, 2004).

Figure 12. The locations of the 1833 and 1866 Nepal earthquakes (stars) as determined using the method outlined in Data and Methods. Contours, the 50% and 67% confidence regions obtained using method described by Bakun (1999); square, previous estimate of epicentral location for the 1833 earthquake from Ambraseys and Douglas (2004); filled circles, locations of felt reports for the 1833 and 1866 earthquakes within 250 km of Kathmandu.

The 2001 Bhuj Earthquake (M_w 7.6)

The 26 January 2001 Bhuj, India, earthquake is the largest calibration event that we used to determine attenuation for cratonic earthquakes and the only cratonic calibration event above magnitude 7 (Fig. 2). Although it appears to be circular reasoning to use our inferred attenuation relation to determine an optimal location and magnitude for this earthquake, this is a potentially interesting exercise because the attenuation relation is primarily constrained by events with $M_w \leq 6$ (Fig. 2). The intensity-derived location for the Bhuj earthquake using intensity values from the Martin and Szeliga (2010) catalog yields a location only 12 km away from the instrumental epicenter. This is slightly larger than the grid spacing (9 km) used in the epicentral location method. However, the magnitude is estimated as M_w 8.0 when using the attenuation relationship derived only from earthquakes in the Indian craton and as M_w 8.6 when using the attenuation relationship derived for all of India. Thus, even though the Bhuj intensities are used to constrain the attenuation relation, the method of Bakun and Wentworth (1997) overpredicts the magnitude of this event by 0.4 or 1.0 M_w units.

To explore why we obtain an unreasonably large magnitude for the Bhuj earthquake (and by implication, an uncertain magnitude for the nearby 1819 Allah Bund earthquake), we examine the intensity values for the 2001 earthquake as a function of distance. The decay in intensity with distance shows a systematic difference with the intensities anticipated by equation (1) for a M_w 7.6 earthquake (Fig. 13). Moderate to small intensity observations are found at significantly greater

distances than those predicted by the attenuation relationship; and, in particular, median intensity observations between 200 km and 875 km (median distances for intensities 4–7) appear between one-half to one intensity unit greater than anticipated.

Four possible explanations for the discrepancy illustrated in Figure 13 are:

1. Intensities for the Bhuj earthquake were systematically overestimated.
2. There is, or can be, a nonlinear dependence of intensities on magnitude for large earthquakes.
3. Intensity observations at regional distances are amplified by the presence of higher-mode surface (Lg) waves.
4. The intensity observations for the Bhuj earthquake indicate a high-Q in the Kachchh Basin.

We shall address each possibility in turn. First, we consider it unlikely that the intensities for the Bhuj earthquake were systematically overestimated. Most of the values for Bhuj in the Martin and Szeliga (2010) catalog are, in fact, systematically lower than the values inferred by Hough et al. (2002), whose intensity assignments were based on media
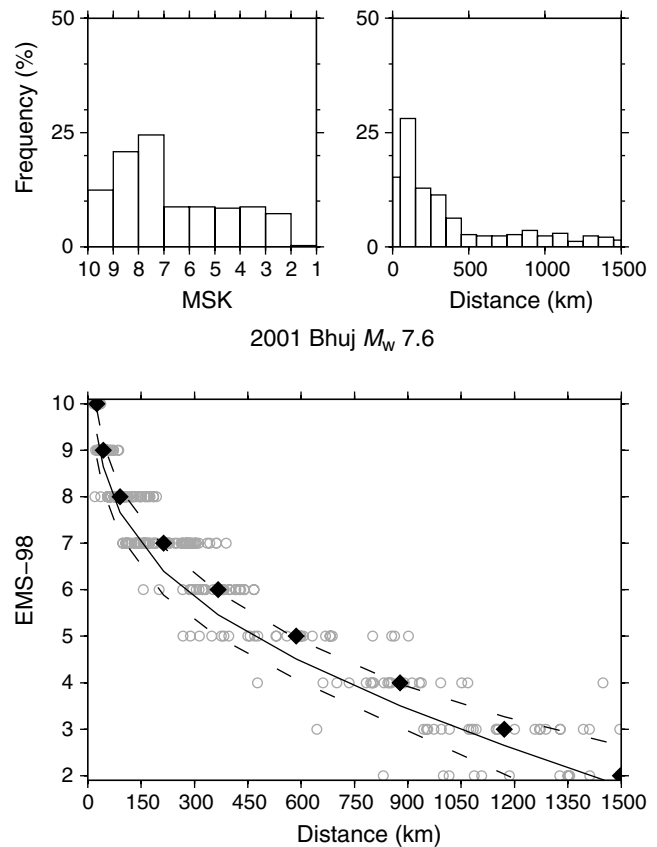
Figure 13. Intensity observations of the 2001 Bhuj M_w 7.6 earthquake compared to the attenuation curve derived for cratonic India for an earthquake of M_w 7.6 (solid line). Open circles, observed intensities; diamonds, median distance for each observed intensity level; dashed lines represent the $2 - \sigma$ envelope of uncertainty in the intensity attenuation model as a function of distance.

reports and have been shown to be biased relative to those estimated from direct surveying of damage (Hough and Pande, 2007).

Second, the functional form of equation (1) is identical to the functional form assumed for attenuation of peak ground acceleration (Evernden *et al.*, 1973). Several studies have shown a good correspondence between intensity and instrumentally determined ground motion measures (e.g., Wald *et al.*, 1999b). One, therefore, might reasonably expect equation (1) to be appropriate for characterizing intensity attenuation for large events. Short of significant nonlinearity associated with ground motions at sediment sites, equation (1) appears to be appropriate for characterization of peak ground acceleration for large and small earthquakes.

Third, when higher-mode surface wavetrains develop and propagate in the continental crust, the highest amplitude shaking typically has a long duration. It is thus reasonable, if not expected, that a prolonged Lg wavetrain with a given peak acceleration will produce a higher intensity observation than will ground motions with the same peak acceleration and a much shorter duration. Shaking duration will clearly be a potential factor for structural damage; it is self-evident that marginally perceptible shaking is more likely to be felt if the strongest amplitudes are prolonged. Clearly, human perception of higher-mode surface waves decreases with distance from the epicenter by a noninteger amount. Thus, a simple, uniform adjustment of intensity observations to correct for amplification is not possible.

Lastly, we can consider the possibility that the intensity distribution reflects especially high-Q in the Kachchh Basin. Bodin *et al.* (2004) calculate Q for the Kachchh Basin using aftershocks of the 2001 Bhuj earthquake and note that their estimates are higher than estimates of Q in northern India calculated by Singh *et al.* (1999). In contrast, in a regional study of Lg attenuation, Pasyanos *et al.* (2009) shows values of Q in the Kachchh Basin to be closer to those measured in northern India (Singh *et al.*, 1999). Additionally, results in Mitra *et al.* (2006) indicate that estimates of Q from the 2001 Bhuj earthquake itself are systematically higher than estimates from other regional events. To test the possibility that the attenuation properties of the Kachchh Basin affect intensity observations and consequently inflate the calculated magnitude of the 2001 Bhuj earthquake, we removed all intensity observations within 200 km of the Bhuj epicenter and inverted for magnitude. The removal of all observations within 200 km of the epicenter results in an increase in epicentral location uncertainty but essentially no change in magnitude. This is not surprising because equation (1) indicates that a change in magnitude will have a larger influence on distant, lower intensity observations than on near-source high intensity observations.

For large earthquakes, locations are well determined where sufficient spatial coverage exists. However, the magnitudes of large events are not well determined using the method outlined in Data and Methods and require consideration. As shown in Figure 13, the intensity values do not generally

match the intensities predicted by equation (1) for an M_w 7.6 earthquake between distances 200 km and 875 km from the epicenter. In addition, the inferred intensity distribution includes moderate intensities to significantly greater distances than the predicted distribution. The lowest felt intensities (II–III) similarly extend farther than predicted. These results suggest that the formation of higher-mode surfaces waves due to long shaking durations in a high-Q environment have amplified intensity observations at regional distances. Simple correction of this amplification is not possible; moreover, these results provide a caution regarding the use of the Bakun and Wentworth (1997) method with an attenuation relation of the form given by equation (1). In particular, if the attenuation relation is constrained largely or entirely by small or moderate earthquakes, the magnitudes estimated for large historical earthquakes can be grossly overestimated.

Discussion

The determination of the magnitudes of historical earthquakes is of interest because, were a complete inventory of historical earthquakes available, we could subject a region to investigations of moment release over space and time. Statistical tests assuming a Gutenberg–Richter distribution of magnitudes show that we are missing 30% of the moderate earthquakes during the period for which most of data are derived (1800–2000). Thus, while moment-release studies can be undertaken for the entire region, they are doomed to be less reliable on a local scale, in particular for the relatively frequent $6.5 \leq M_w \leq 7.5$ events that are typically important for controlling probabilistic hazard.

The caveat discussed in the previous section, that our attenuation findings for small earthquakes do not provide satisfactory predictions for the attenuation observed in the largest earthquakes and therefore yield unsatisfactory magnitude predictions, is perceived to be a substantial problem in India because it is for these largest earthquakes that reliable magnitude information is most needed. It is possible that a similar problem exists with the intensity relations established for North America.

Epicentral locations determined using the methods we describe show demonstrable scatter. One question that arises in the determination of magnitude and epicentral location for early earthquakes is what constitutes an acceptable determination of these parameters. If we are interested in establishing an inventory of potentially active faults, we should presumably prefer locations that lie within one source dimension (e.g., a fault rupture length) of the earthquake. If we are interested in identifying segments of those faults that remain unruptured, we require yet higher accuracy. It is clear from the analysis we present here that few of our post-1950 solutions for earthquakes with $M_w < 6$ are within one fault length of the instrumental epicenter, and, by implication, we must assume that the same is true of the earthquakes earlier in the catalog.

For many of the events in the catalog with poor intensity coverage, we do not attempt to determine a location using

quantitative methods. Yet even for these earthquakes we recognize that the approximate location and its intensity data are of utility in seismic hazard studies. Martin and Szeliga (2010) utilize this information to map maximum shaking intensity encountered in a grid throughout India.

In general, for larger earthquakes ($7 < M_w < 8$) where rupture lengths range from 30 km to 300 km, we find that our preferred location lies near or above the inferred rupture surface; however, we note that, even for some very large earthquakes in the catalog, the dimensions and location of the rupture zone remain enigmatic (e.g., the Chittagong 1762 and Bihar-Nepal 1934 earthquakes).

For 100 earthquakes in the instrumental period (post-1950) for which we have both epicentral parameters and intensity data, we find that fewer than 30% of these earthquakes can be located to within one fault length of the true epicenter using intensity data. The median mislocation error using the method of Bakun and Wentworth (1997) exceeds 100 km; however, choosing the minimum magnitude location instead of the minimum deviation location reduces the misfit by a factor of 2. The reason for the poor performance of the algorithm is partly due to the small number of observations available for many of these earthquakes, as well as the small dynamic range of the intensity observations for each earthquake. We conclude the algorithm cannot be expected to do better for historical earthquakes; location accuracies are likely to be no better than 50 km. One disappointing result is that, from the data alone, there seems to be no reliable way to characterize the quality of each solution. In general, earthquakes with fewer than 10 locations gave consistently unreliable locations. We found that the most unreliable solutions were those where large differences were found between the minimum deviation location and the minimum magnitude location. The best locations were found to be those in which these two locations agreed to within 30 km, but this applies to fewer than 30% of the data.

Conclusions

Newly available intensity observations for India provide a wealth of material for evaluating the location and magnitude of numerous earthquakes that have hitherto been amenable only to qualitative analysis and, in particular, permit us to assess attenuation throughout the subcontinent. We use an attenuation relation derived from modern (post-1950) earthquakes with well-determined instrumental locations and the method of Bakun and Wentworth (1997) to estimate the optimal locations and magnitudes for 181 historical earthquakes, with case studies of large events in 1803, 1819, 1833, and 1866.

Of particular interest are the characteristic attenuation-versus-distance parameters for India. We quantify attenuation for all Indian earthquakes and separately for plate boundary events (Himalaya) and cratonic events. We find that intensity attenuation in the Himalaya region is comparable to that in California, while attenuation in cratonic India is significantly higher than attenuation in the central/eastern United States.

One unexpected finding is that, for the largest of the cratonic earthquakes (Bhuj 2001 and Allah Bund 1819), our attenuation relation significantly overestimates the magnitudes estimated from instrumental and/or geological constraints. This results from shaking being felt more strongly out to greater distances than expected by our attenuation relationship. We suggest that this may be a systematic effect that is common to all attenuation models. The distant shaking from large earthquakes is not simply not well characterized by shaking from small earthquakes. We propose that the duration of L_g shaking at large distances may be responsible for this effect.

Our search for uncertainty criteria to describe location accuracy is unsatisfactory in that we have found no objective method from the intensity data alone to quantify the accuracy of our solutions. Where more than 100 intensity values are available, the solution is usually within 30 km of the true epicenter. This criterion applies to only 16 events, less than 3% of the catalog. Where the minimum deviation and minimum magnitude solution are close, the calculated epicenter is usually within 30 km of the instrumental location, but even this condition applies to less than 30% of the instrumental catalog and, by extension, to fewer than 177 of the 570 earthquakes in the entire catalog.

The magnitudes of earthquakes in the instrumental period were not well characterized by the Bakun and Wentworth (1997) algorithm. This is perhaps not too surprising because the assigned magnitude for a given attenuation depends on distance, which as summarized previously shows a large range of mislocation errors. Magnitudes were in general overestimated by a median mismatch of 0.4 for the 100 earthquakes for which instrumental magnitudes were known. The median magnitude misfit using the minimum magnitude location underpredicts the instrumental magnitude by M_w 0.6. Again, this uncertainty in magnitude suggests that historical earthquakes cannot be characterized to better than $M_w \pm 0.5$ from the historical data analyzed here.

Data and Resources

Intensity distributions for moderate and large earthquakes occurring on the Indian subcontinent are available from the Amateur Seismic Centre (http://www.asc-india.org). Data from the Global Centroid Moment Tensor Project was retrieved from http://www.globalcmt.org; ISC and MHDF catalog data were retrieved using SeismiQuery www.iris.edu/dms/sq.htm. Figure 9 was created using gnuplot (http://www.gnuplot. info/); all other figures were created using Generic Mapping Tools (Wessel and Smith, 1998).

Acknowledgments

References

Ambraseys, N. (2004). Three little known early earthquakes in India, *Curr. Sci. India* **86,** no. 4, 506–508.

Ambraseys, N., and J. J. Douglas (2004). Magnitude calibration of north Indian earthquakes, *Geophys. J. Int.* **159,** 165–206, doi 10.1111/j.1365-246X.2004.02323.x.

Ambraseys, N., and D. Jackson (2003). A note on early earthquakes in northern India and southern Tibet, *Curr. Sci. India* **84,** no. 4, 570–582.

Atkinson, G. M., and D. J. Wald (2007). "Did You Feel It?" intensity data: A surprisingly good measure of earthquake ground motion, *Seismol. Res. Lett.* **78,** no. 3, 362–368.

Bakun, W. H. (1999). Erratum to estimating earthquake location and magnitude from seismic intensity data, *Bull. Seismol. Soc. Am.* **79,** 557.

Bakun, W. H., and A. McGarr (2002). Differences in attenuation among the stable continental regions, *Geophys. Res. Lett.* **29,** no. 23, 2121, doi 10.1029/2002GL015457.

Bakun, W. H., and C. M. Wentworth (1997). Estimating earthquake location and magnitude from seismic intensity data, *Bull. Seismol. Soc. Am.* **87,** no. 6, 1502–1521.

Bakun, W. H., A. C. Johnston, and M. G. Hopper (2003). Estimating locations and magnitudes of earthquakes in eastern North America from modified Mercalli intensities, *Bull. Seismol. Soc. Am.* **93,** no. 1, 190–202.

Båth, M. (1965). Lateral inhomogeneities of the upper mantle, *Tectonophysics* **2,** no. 6, 483–514.

Bender, B. (1983). Maximum likelihood estimation of *b* values for magnitude grouped data, *Bull. Seismol. Soc. Am.* **73,** no. 3, 831–851.

Bilham, R. (1995). Location and magnitude of the 1833 Nepal earthquake and its relation to the rupture zones of contiguous Great Himalayan earthquakes, *Curr. Sci. India* **69,** no. 2, 101–128.

Bilham, R. (1998). Slip parameters for the Rann of Kachchh, India, 16 June 1819, earthquake, quantified from contemporary accounts, in *Coastal Tectonics, Special Publications*, I. S. Stewart and C. Vita-Finzi (Editors), Vol. **146**, Geological Society, London, 295–319.

Bodin, P., L. Malagnini, and A. Akinci (2004). Ground-motion scaling in the Kachchh Basin, India, deduced from aftershocks of the 2001 M_w 7.6 Bhuj earthquake, *Bull. Seismol. Soc. Am.* **94,** no. 5, 1658–1669.

Burnes, A. (1835). A memoir on the eastern branch of the River Indus giving an account of the alterations produced by it by an earthquake in 1819, also a theory of the Runn, and some conjectures on the route of Alexander the Great, drawn up in the years 1827–1828, *R. Asiat. Soc.* **3,** 550–588.

Chen, W.-P., and P. Molnar (1977). Seismic moments of major earthquakes and the average rate of slip in central Asia, *J. Geophys. Res.* **82,** no. 20, 2945–2969.

Efron, B., and R. J. Tibshirani (1993). *An Introduction to the Bootstrap*, Chapman and Hall/CRC, New York.

Ellis, M., J. Gomberg, and E. Schweig (2001). Indian earthquake may serve as analog for New Madrid earthquakes, *Eos Trans. AGU* **82,** no. 32, 345–347.

Engdahl, E. R., and A. Villasenor (2002). Global seismicity: 1900–1999, in *International Handbook of Earthquake and Engineering Seismology*, W. H. K. Lee, H. Kanamori, P. C. Jennings, and C. Kisslinger (Editors), Vol. **A**, chap. 41, Academic Press, Boston, 665–690.

Evernden, J. F., R. R. Hibbard, and J. F. Schneider (1973). Interpretation of seismic intensity data, *Bull. Seismol. Soc. Am.* **63,** no. 2, 399–422.

Frankel, A. D. (1994). Implications of felt area–magnitude relations for earthquake scaling and the average frequency of perceptible ground motion, *Bull. Seismol. Soc. Am.* **84,** no. 2, 462–465.

Grünthal, G. and A. Levret (Editors) (2001). *European Macroseismic Scale 1998 (EMS-98), Cahiers du Centre Européen de Géodynamique et de Séismologie*, Vol. **15**, Joseph Beffort, Helfent-Bertrange, Luxembourg.

Gupta, S., S. S. Rai, K. S. Prakasam, D. Srinagesh, B. K. Bansal, R. K. Chadha, K. Priestley, and V. K. Gaur (2003). The nature of the crust in southern India: Implications for Precambrian crustal evolution, *Geophys. Res. Lett.* **30,** no. 8, 1419, doi 10.1029/2002GL016770.

Gutenberg, B., and C. F. Richter (1954). *The Seismicity of the Earth and Associated Phenomena*, Princeton University Press, Princeton, New Jersey.

Hough, S. E., and P. Pande (2007). Quantifying the media bias in intensity surveys: Lessons from the 2001 Bhuj, India, earthquake, *Bull. Seismol. Soc. Am.* **97,** no. 2, 638–645, doi 10.1785/0120060072.

Hough, S. E., S. Martin, R. Bilham, and G. M. Atkinson (2002). The 26 January 2001 *M* 7.6 Bhuj, India, earthquake observd and predicted ground motion, *Bull. Seismol. Soc. Am.*, **92,** no. 6, 2061–2079.

Howell, B. F., and T. R. Schultz (1975). Attenuation of modified Mercalli intensity with distance from the epicenter, *Bull. Seismol. Soc. Am.* **65,** no. 3, 651–665.

Jade, S., B. C. Bhatt, Z. Yang, R. Bendick, V. K. Gaur, P. Molnar, M. B. Anand, and D. Kumar (2004). GPS measurments form the Ladakh Himalaya, India: Preliminary tests of plate-like or continuous deformation in Tibet, *Geol. Soc. Am. Bull.* **116,** no. 11/12, 1385–1391, doi 10.1130/B25357.1.

Johnston, A. C. (1996). Seismic moment assessment of earthquakes in stable continental regions—II. Historical seismicity, *Geophys. J. Int.* **125,** no. 3, 639–678.

Joyner, W. B., and D. M. Boore (1993). Methods for regression analysis of strong-motion data, *Bull. Seismol. Soc. Am.* **83,** no. 2, 469–487.

Khattri, K. N. (1987). Great earthquakes, seismicity gaps and potential for earthquake disaster along the Himalayan plate boundary, *Tectonophysics* **138,** 79–92.

Khattri, K. N., and A. K. Tyagi (1983). Seismicity patterns in the Himalayan plate boundary and identification of the areas of high seismic potential, *Tectonophysics*, **96,** 281–297.

Kumar, S., S. G. Wesnousky, T. K. Rockwell, R. W. Briggs, V. C. Thakur, and R. Jayangondaperumal (2006). Paleoseismic evidence of great surface rupture earthquakes along the Indian Himalaya, *J. Geophys. Res.* **111,** B03304.

Lavé, J., D. Yule, S. Sopkota, K. Basant, C. Madden, M. Attal, and R. Pandey (2005). Evidence for a great medieval earthquake (~1100 A.D.) in the central Himalayas, Nepal, *Science* **307,** 1302–1305.

MacMurdo, J. (1823). Papers relating to the earthquake which occurred in India in 1819, *Lit. Soc. Bombay Trans.* **3,** 90–116.

Malik, J. N., T. Nakata, H. Sato, T. Imaizumi, T. Yoshioka, G. Philip, A. K. Mahajan, and R. V. Karanth (2001). January 26, 2001, the Republic Day (Bhuj) earthquake of Kachchh and active faults, Gujarat, western India, *J. Act. Fault Res., Jpn.* **20,** 112–126.

Mallet, R., and J. W. Mallet (1858). The earthquake catalogue of the British Association with the discussion, curves, and maps, etc., *Trans. Br. Assoc. Adv. Sci., 1852–1858,* Taylor and Francis, London.

Martin, S., and W. Szeliga (2010). A catalog of felt intensity data for 589 earthquakes in India, 1636–2008, *Bull. Seismol. Soc. Am.* **100**, no. 2, 562–569.

Miao, Q., and C. A. Langston (2008). Comparative study of distance attenuation in Central United States and Western India, *Seismol. Res. Lett.* **79,** no. 3, 446–456.

Mitra, S., K. F. Priestley, V. K. Gaur, and S. S. Rai (2006). Frequency dependent *Lg* attenuation in the Indian platform, *Bull. Seismol. Soc. Am.* **96,** no. 6, 2449–2456, doi 10.1785/0120050152.

Monsalve, G., A. F. Sheehan, C. Rowe, and S. Rajaure (2008). Seismic structure of the crust and upper mantle beneath the Himalayas: Evidence for eclogitization of lower crustal rocks in the Indian Plate, *J. Geophys. Res.* **113,** no. B08315, doi 10.1029/2007JB005424.

Oldham, R. D. (1926). The Cutch (Kachh) earthquake of 16th June 1819 with a revision of the great earthquake of 12th June 1897, *Memoir. Geol. Surv. India,* **46,** 71–177.

Oldham, T. (1883). A catalogue of Indian earthquakes from the earliest time to the end of A.D. 1869, *Memoir. Geol. Surv. India* **29,** 163–215.

Ortiz, M., and R. Bilham (2003). Source area and rupture parameters of the 31 December 1881 $M_w = 7.9$ Car Nicobar earthquake estimated from

tsunamis recorded in the Bay of Bengal, *J. Geophys. Res.* **108,** no. 4, 2215, doi 10.1029/2002JB001941.

Pande, P. and J. R. Kayal (Editors) (2003). *Kutch (Bhuj) earthquake 26 January 2001*, no. 76 in Special Publications, Geological Survey of India, Kolkata.

Pasyanos, M. E., E. M. Matzel, W. R. Walter, and A. J. Rodgers (2009). Broad-band *Lg* attenuation modelling in the Middle East, *Geophys. J. Int.* **177,** no. 3, 1166–1176, doi 10.1111/j.1365-246X.2009.04128.x.

Rajendran, C. P., and K. Rajendran (2001). Characteristics of deformation and past seismicity associated with the 1819 Kutch earthquake, north-western India, *Bull. Seismol. Soc. Am.* **91,** no. 3, 407–426.

Rajendran, C. P., and K. Rajendran (2005). The status of central seismic gap: A perspective based on the spatial and temporal aspects of the large Himalayan earthquakes, *Tectonophysics* **395,** 19–39.

Schmidt, D. A., and R. Bürgmann (2006). InSAR constraints on the source parameters of the 2001 Bhuj earthquake, *Geophys. Res. Lett.* **33,** L02315, doi 10.1029/2005GL025109.

Seeber, L., and J. G. Armbruster (1981). Great detachment earthquakes along the Himalayan arc and long-term forecasting, in *Earthquake Prediction—An International Review*, Maurice Ewing Series 4, D. W. Simpson and P. G. Richards (Editors), American Geophysical Union, Washington, D.C.,259–277.

Singh, S. K., R. S. Dattatrayam, and H. K. Gupta (1999). A spectral analysis of the 21 May 1997, Jabalpur, India, earthquake ($M_w = 5.8$) and estimation of ground motion from future earthquakes in the Indian shield region, *Bull. Seismol. Soc. Am.* **89,** no. 6, 1620–1630.

Talwani, P., and A. Gangopadhyay (2000). Schematic model for intraplate earthquakes, Fall meeting supplement, abstract S21C–10, *Eos Trans. AGU* **81,** no. 48.

Wald, D. J., V. Quitoriano, L. Dengler, and J. Dewey (1999a). Utilization of the Internet for rapid community intensity maps, *Seismol. Res. Lett.* **70,** no. 6, 680–697.

Wald, D. J., V. Quitoriano, T. H. Heaton, and H. Kanamori (1999b). Relationships between peak ground acceleration, peak ground velocity, and modified Mercalli intensity in California, *Earthq. Spectra* **15,** no. 3, 557–564.

Wessel, P., and W. H. F. Smith (1998). New improved version of Generic Mapping Tools released, *Eos Trans. AGU* **79,** 579.

Wyss, M. (1979). Estimating maximum expectable magnitude of earthquakes from fault dimensions, *Geology* **7,** no. 7, 336–340.

Cooperative Institute for Research in Environmental Sciences (CIRES) and Department of Geological Sciences
University of Colorado at Boulder
Boulder, Colorado
   (W.S.)

U. S. Geological Survey
Pasadena, California
   (S.H.)

Victoria University of Wellington
School of Geography, Environment, and Earth Sciences
Wellington, New Zealand
   (S.M.)

CIRES and Department of Geological Sciences
University of Colorado at Boulder
Boulder, Colorado
   (R.B.)